Tanabe, T., Nukada, T., Nishikawa, Y., Sugimoto, K., Suzuki, H., Takahashi, H., Noda, M., Haga, T., Ichiyama, A., Kangawa, K., Minamino, N., Matsuo, H., & Numa, S. (1985) *Nature (London) 315*, 242-245.
Tsai, S.-C., Adamik, R., Kanaho, Y., Halpern, J. L., & Moss, J. (1987) *Biochemistry 26*, 4728-4733.
Van Meurs, K. P., Angus, C. W., Lavu, S., Kung, H.-F., Czarnecki, S., Moss, J., & Vaughan, M. (1987) *Proc. Natl. Acad. Sci. U.S.A. 84*, 3107-3111.
Weinstein, L. S., Spiegel, A. M., & Carter, A. D. (1988) *FEBS Lett. 232*, 333-340.
Weisgraber, K. H., Newhouse, Y. M., & Mahley, R. W. (1988) *Biochem. Biophys. Res. Commun. 157*, 1212-1217.
Worley, P. F., Baraban, J. M., Van Dop, C., Neer, E. J., & Snyder, S. H. (1986) *Proc. Natl. Acad. Sci. U.S.A. 83*, 4561-4565.
Yatsunami, K., & Khorana, H. B. (1985) *Proc. Natl. Acad. Sci. U.S.A. 82*, 4316-4320.

NMR Comparison of Prokaryotic and Eukaryotic Cytochromes *c*†

Mei-Hing Chau, Meng Li Cai, and Russell Timkovich*
Department of Chemistry, University of Alabama, Tuscaloosa, Alabama 35687-0336
Received October 27, 1989; Revised Manuscript Received January 30, 1990

ABSTRACT: ^{1}H NMR spectroscopy has been used to examine ferrocytochrome *c*-551 from *Pseudomonas aeruginosa* (ATCC 19429) over the pH range 3.5–10.6 and the temperature range 4–60 °C. Resonance assignments are proposed for main-chain and side-chain protons. Comparison of results for cytochrome *c*-551 to recently assigned spectra for horse cytochrome *c* (Wand et al. (1989) *Biochemistry 28*, 186–194) and mutants of yeast iso-1 cytochrome (Pielak et al. (1988) *Eur. J. Biochem. 177*, 167–177) reveals some unique resonances with unusual chemical shifts in all cytochromes that may serve as markers for the heme region. Results for cytochrome *c*-551 indicate that in the smaller prokaryotic cytochrome, all benzoid side chains are rapidly flipping on the NMR time scale. In contrast, in eukaryotic cytochromes there are some rings flipping slowly on the NMR time scale. The ferrocytochrome *c*-551 undergoes a transition linked to pH with a p*K* around 7. The pH behavior of assigned resonances provides evidence that the site of protonation is the inner or buried 17-propionic acid heme substituent (IUPAC-IUB porphyrin nomenclature). Conformational heterogeneity has been observed for segments near the inner heme propionate substituent.

Cytochrome *c* is a well-known component of respiratory electron transport chains where it transfers electrons to a terminal oxidase. Its structure is highly conserved in eukaryotes. It has usually 102–103 residues in higher eukaryotes and up to 116 in lower eukaryotes and plants, which can have a variable N-terminal extension. The ca. 100-residue core has high sequence homology, and the crystal structures from horse, tuna, bonito, and yeast show a tightly conserved tertiary structure. In prokaryotes, a functionally equivalent electron-transport protein is found, but there can be large variations in size and sequence (Dickerson & Timkovich, 1975; Timkovich, 1979; Meyer & Kamen, 1982). Cyt *c*-551[1] from *Pseudomonas aeruginosa* is an example of a bacterial cytochrome of smaller size (82 residues). It donates electrons to membrane oxidases during the aerobic respiration of *Pseudomonads* or to a dissimilatory nitrite reductase during anaerobic respiration. The amino acid sequence (Ambler, 1963a,b) and X-ray crystal structure (Dickerson et al., 1976; Almassy & Dickerson, 1978; Matsuura et al., 1982) have been determined. Critical structural differences compared to eukaryotic cytochromes include deletions around the bottom of the heme crevice, a major reorientation of the invariant tryptophan found hydrogen bonding to the buried heme propionate groups, and a novel polyproline-type helix that positions the sixth ligand methionine for iron coordination. Cyt *c*-551 also demonstrates functional differences compared to cyt *c*. Its reduction potential is sensitive to pH and linked to a pH-controlled transition with a p*K* around 7 (Moore & Williams, 1977; Moore et al., 1980), while that of eukaryotic cytochromes *c* is independent of pH for several units around neutrality. Its rate of electron self-exchange is more than 3 orders of magnitude faster than for cyt *c* (Timkovich et al., 1988, and references therein). There is evidence that its association with redox partners may rely more on hydrophobic interactions than for cyt *c* (Timkovich, 1986).

Recently, extensive ^{1}H NMR studies have been reported for the eukaryotic horse cyt *c* (Wand et al., 1989), and the Thr 102 and Phe 82 mutants of eukaryotic yeast iso-1 cyt *c* (Pielak et al., 1989a,b). Investigation of the spectrum of *P. aeruginosa* cyt *c*-551 in its ferrous oxidation state affords an opportunity to compare structure and spectra between the larger eukaryotic cytochromes and the smaller prokaryotic version. *Pseudomonas aeruginosa* cyt *c*-551 has been studied previously by ^{1}H NMR and select assignments have been made (Keller & Wüthrich, 1976; Moore et al., 1977; Keller & Wüthrich, 1978; Chao et al., 1979; Senn et al., 1980). This article proposes extensive assignments for the ferrocytochrome

† Financial support was provided in part by NIH Grant GM36264. This work was completed in partial fulfillment of the Ph.D. degree requirements of M. H. Chau. A preliminary account of these results has been presented at the American Chemical Society Southeast Regional Meeting, Louisville, KY, 1987.
* To whom correspondence should be addressed.

[1] Abbreviations: cyt, cytochrome; DQF-COSY, double-quantum filtered correlation spectroscopy; NOESY, nuclear Overhauser enhancement correlation spectroscopy; NOE, nuclear Overhauser enhancement; HOHAHA, homonuclear Hartmann-Hahn spectroscopy; TPPI, time proportional phase incrementation.

0006-2960/90/0429-5076$02.50/0

especially of main-chain protons but also of many of the side-chain protons. These assignments and the behavior of the resonances to experimental variations afford structural insights not previously available from the crystal structure.

Materials and Methods

Cyt *c*-551 was purified from *Pseudomonas aeruginosa* strain ATCC 19429 by methods previously described (Timkovich et al., 1982). Protein was dialyzed versus 50 mM ammonium bicarbonate and lyophylyzed. NMR samples were dissolved in either 99.98%: ^2H_2O or 90% ^1H_2O/10% ^2H_2O buffered to the appropriate pH with either 50 or 100 mM potassium phosphate. No discernible spectral differences were seen between these buffer concentrations. After dissolution, the pH was checked with a microelectrode calibrated against normal protic standards. It was adjusted if needed with stock solutions of acid or base. Protein concentrations were in the range 1.5–10 mM. Ferrocytochrome *c*-551 is subject to severe line broadening due to chemical exchange in the presence of even trace amounts of ferricytochrome (Timkovich et al., 1988, and references therein). Samples of ferricytochrome at the desired pH were deoxygenated in the NMR tube by cycles of vacuum degassing and argon flushing. Under an argon blanket, a preweighed amount of sodium dithionite, typically 1–2 mg, was added. Control experiments established this was insufficient to perturb the pH at 50–100 mM buffer more than 0.1 units at any pH value studied. After several additional cycles of vacuum and argon, the tube was sealed with a microtorch. The line widths of indicator resonances were checked to ensure complete reduction. For example, the line width of the Met 61 sulfur methyl is on the order of 4–7 Hz (depending upon shimming) at 60 °C for completely reduced protein. Ferrocytochrome samples prepared in this way are stable and can be heated to 60 °C without any obvious precipitation or changes in line widths for resolved resonances. It will be shown that long-term storage does lead to subtle changes that can be detected by two-dimensional scalar correlation spectroscopy. Solutions of the ferricytochrome are labile and show progressive line broadening with time, even at 4 °C. This has also been reported by others (Chao et al., 1979). In dilute solutions, ferrocytochrome *c*-551 is stable to pH values as low as 3, but in concentrated solutions the pH could not be lowered below 3.5. At lower values, instability was manifested by difficulty in maintaining complete reduction, even in sealed tubes.

Spectra were recorded at 360 and 500 MHz on Bruker AM instruments. Chemical shifts to be reported came from 500-MHz data sets with dioxane at 3.74 ppm as internal standard. A convenient reference peak in the protein is the 20-meso-proton which resonates at 9.22 ± 0.01 ppm independent of pH or temperature over a wide range. Shifts for nonresolved protons were taken from cross peaks. After zero-filling and Gaussian apodization, shifts could be measured to ±0.01 ppm. All two-dimensional spectra were recorded in the phase-sensitive mode by the TPPI method (Marion & Wüthrich, 1983). The hardware receiver phase (Marion & Bax, 1988) and the delay before the first data point of any free induction decay (Hoult et al., 1983) were adjusted to produce the flattest possible base line. Free induction decays were adjusted by a linear base-line correction prior to Fourier transformation. For some spectra, a linear base-line correction was applied after transformation to F2 but prior to transformation to F1 to remove small residual base-line tilt and offset. For some final spectra, slices parallel to F2 were corrected by polynomial functions fitted to the base line to improve the final appearance in contour plots.

DQF-COSY spectra (Rance et al., 1984) were recorded with the SCUBA sequence for suppression of the solvent peak (Brown et al., 1988). NOESY (Macura et al., 1981) spectra in ^2H_2O were recorded with preirradiation of the residual water with the irradiation both frequency and phase locked to the observe transmitter. In ^1H_2O buffers, NOESY spectra were recorded with SCUBA presaturation or with a jump-and-return echo pulse as the final observe pulse [ECHO NOESY, Sklenar and Bax (1987)]. This was to check against loss of intensity for labile NH protons because of saturation transfer with the solvent. In practice, it was found that this was not a serious problem. NOESY spectra were examined for mixing times of 50, 75, 100, 150, and 200 ms. A mixing time of 150 ms produced the strongest cross-peak intensities with only minimal spin-diffusion peaks. HOHAHA spectra in ^2H_2O or ^1H_2O were recorded with a WALTZ-17 sequence (Bax & Davis, 1985; Driscoll et al., 1989). Mixing times were 14, 40, 55, and 72 ms for investigating direct coupling and relayed coupling. Digital resolution in F2 was typically 3.6 Hz per point and in F1, 14 Hz per point before zero-filling, 3.6 Hz per point afterward. Apodization functions were varied to improve the appearance of plots. Typically, sine-squared window functions were employed with phase shifts of 60–36° for DQF-COSY spectra. Gaussian window functions (negative line broadening of 25 Hz with the free induction decay envelope reaching a maximum at ca. 6 ms) were applied to F2 dimensions for HOHAHA and NOESY spectra. Spectra were examined at pH values from 3.09 to 10.6. Temperatures examined ranged from 4 to 60 °C. The temperature and pH variation was important and helped to resolve NH protons overlapping at a single set of conditions. However, only at pH values of 5 and below was the amide exchange rate slow enough to observe all backbone amide resonances. The α-protons and other side-chain protons were in general not sensitive to temperature and pH.

The effects of protonation on the chemical shifts of the heme propionate side chains were measured for free heme to provide a model for behavior in the protein. Commercial hemin (Fe^{3+} protoporphyrin IX chloride) was dissolved in deuterated dimethyl sulfoxide and deuterium oxide was added to a final concentration of 25% (v/v). The acidity was adjusted by the addition of either ^2HCl or NaO^2H. CO was bubbled through the solution for several minutes to remove oxygen and provide a saturating solution of CO. Under a blanket of CO, minimal solid sodium dithionite was added and the solution turned bright red, indicative of formation of the ferrous CO heme complex. The solution was transferred by syringe to septum-capped NMR tubes previously flushed with CO and the spectrum recorded.

Crystal structure coordinates of *P. aeruginosa* are available from the Brookhaven Protein Data Bank. These were examined with the aid of the SYBYL graphics display and molecular modeling software of Tripos Associates, St. Louis.

Results and Discussion

The proposed assignments for *Pseudomonas aeruginosa* ferrocytochrome *c*-551 are summarized in Table I, special resonances with more than one shift value are given in Table II, and a summary of NOE connections in Table III. The assignment of proton two-dimensional spectra of proteins has been discussed by many authors (Englander & Wand, 1987) and reviewed in a monograph (Wüthrich, 1986). The general strategy in the present case may be outlined as follows. One-dimensional spectra were surveyed over a wide range of temperature and pH to check protein purity, determine feasible temperature and pH conditions, and measure the chemical

Table I: Assignments for *Pseudomonas aeruginosa* Ferrocytochrome *c*-551[a]

residue	NH 32 °C	NH 60 °C	C_α	C_β	C_γ	C_δ	others
Glu 1			4.01	2.02			
Asp 2	8.97	8.13	4.84	2.59			
Pro 3			4.21	2.13		3.65	
				1.57		3.90	
Glu 4	7.91	7.94	3.30	1.95	2.36		
Val 5	7.04	7.05	3.68	2.19	1.01		
					0.96		
Leu 6	7.57	7.49	4.05	2.01	1.72	0.91	
				1.32		0.93	
Phe 7	8.32	8.25	4.28	2.92			C2 + 6 7.24
				3.00			C3 + 5 6.91
							C4 7.07
Lys 8	6.96	6.95	3.91	1.88	1.30		
				1.70			
Asn 9	8.80	8.71	4.63	2.89[b]			
Lys 10	8.95	8.85	4.80	2.54	1.78		
				2.22			
Gly 11	7.91	7.79	4.70				
			3.97				
Cys 12	8.49	8.45	4.94	3.28			
				3.01			
Val 13	6.63	6.58	3.61	1.03	0.64		
					0.85		
Ala 14	7.36	7.36	4.10	1.77			
Cys 15	6.88	6.81	4.32	0.96			
				1.84			
His 16	6.80	6.77	3.64	0.87			N_π 8.63
				0.21			C2 0.63
							C5 0.73
Ala 17	7.70	7.53	4.21	1.22			
Ile 18	8.13	8.11	3.17	1.59	0.62 CH_3	0.55 CH_3	
					0.80		
					1.25		
Asp 19	8.20	7.95	4.46	2.46[c]			
Thr 20	6.46	6.47	4.36	3.70	0.89		
Lys 21	8.43	8.18	3.55	1.65[d]	1.08[e]	1.52	C_ϵ 2.82, NH_3^+ 7.50
						1.62	C_ϵ 2.95
Met 22	7.35	7.23	4.37	1.27	1.93		SCH_3 2.30
					1.52		
Val 23	6.95	6.86	3.93	1.84	1.55		
					1.14		
Gly 24	6.71	6.60	3.71				
			0.13				
Pro 25			3.57	0.97	0.10	2.90	
				0.52	0.32	2.10	
Ala 26	8.45	8.22	3.79	0.68			
Tyr 27	7.50	7.43	4.06	2.33			C2 + 6 5.78
				2.70			C3 + 5 4.53
Lys 28	8.93	8.71	3.90[f]	1.76	1.22	3.61	
				1.54	1.28		
Asp 29	6.83	6.72	4.62	2.62			
				2.73			
Val 30	7.55	7.49	4.15	2.20	1.53		
					0.70		
Ala 31	8.59	8.50	4.02	1.58			
Ala 32	7.55	7.55	4.16	1.59			
Lys 33	7.86	7.77	4.08	1.91	1.07		
				2.02	1.23		
Phe 34	7.75	7.76	4.63	2.76			C2 + 6[g] 7.63
				3.43			C3 + 5 7.66
							C4 7.62
Ala 35	7.78	7.87	4.21	1.55			
Gly 36	8.83	8.64	4.07				
			3.90				
Gln 37	7.83	7.79	4.52	2.25	2.40		
Ala 38	8.99	8.69	4.30	1.47			
Gly 39	9.02	8.85	4.10[h]				
Ala 40	7.65	7.64	4.11	1.65			
Glu 41	8.72	8.81	3.67	2.04	2.26		
				2.06	2.46		
Ala 42	7.93	7.59	4.11	1.44			
Glu 43	7.80	7.65	4.09	1.95	2.15		
				2.33			
Leu 44	8.69	8.53	3.92	1.94	1.73	0.80	
				1.39		0.85	

Table I (Continued)

residue	NH 32 °C	NH 60 °C	C_α	C_β	C_γ	C_δ	others
Gln 46	7.38	7.37	3.84	2.16	2.43		
				2.37			
Arg 47	7.55	7.60	3.73	1.73	1.76	3.16	N_ϵ 7.27
				0.85	1.83	3.09	
Ile 48	8.17	8.01	1.51	1.66	0.67 CH_3	1.32[i]	
					1.01		
					1.76		
Lys 49	7.09	7.04	3.85	1.60	1.24		
				1.37			
Asn 50	8.05	7.97	4.49	2.59[j]			
Gly 51	7.39	7.28	3.61				
			2.02				
Ser 52	7.19	7.10	4.26	2.82[k]			
Gln 53	7.88	7.74	4.33	1.90	2.22		NH_2 6.78, 7.41
Gly 54	8.40	8.25	4.22				
			3.90				
Val 55	10.35	10.25	3.82	2.47	1.04		
					0.69		
Trp 56	10.71	10.62	4.64	3.65			C2 7.74
				3.83			C4 8.02
							C5 7.28
							C6 7.13
							C7 7.60
							indole 11.23
Gly 57	7.93	7.94	4.59				
			4.15				
Pro 58			4.27	2.63		3.95	
				2.34		3.66	
Ile 59	7.47	7.37	4.68	2.16	1.32 CH_3	1.13	
					1.50		
					1.82		
Pro 60			4.87	1.99			
				1.52			
Met 61	8.74	8.62	3.65	−0.89	−0.48		SCH_3 −2.94
				−2.73	−3.55		
Pro 62			4.78	2.22		2.95	
				1.24		3.74	
Pro 63			3.85	2.50			
				1.73			
Asn 64	6.94	6.90	4.83	2.44			NH_2 7.23, 3.19
				2.10			
Ala 65	8.78	8.56	4.51	1.33			
Val 66	7.72	7.59	4.85	2.43	0.63		
					0.74		
Ser 67	8.53	9.06	4.59	3.93			
				4.40			
Asp 68	9.05	8.76	4.32	2.64			
Asp 69	8.61	8.32	4.41	2.62[l]			
Glu 70	7.85	7.72	3.84	2.51	2.34		
				1.69			
Ala 71	8.83	8.69	3.93	1.63			
Gln 72	8.14	8.08	3.99[m]	2.22	2.53		
				2.38			
Thr 73	8.21	8.12	3.93	4.30	1.23		
Leu 74	8.66	8.54	4.31	2.34	1.80	1.20	
				1.73		1.24	
Ala 75	8.80	8.73	3.95	1.57			
Lys 76	8.20	8.08	3.91	1.99			
				1.49			
Trp 77	7.83	7.87	4.37	3.56			C2 7.27
				3.22			C4 7.35
							C5 6.37
							C6 5.82
							C7 7.06
							indole 10.00
Val 78	9.27	9.04	2.60	2.22	0.65		
					0.52		
Leu 79	7.71	7.62	3.86	1.92	1.85	0.85	
				1.58		0.93	
Ser 80	7.47	7.44	4.45	4.00[n]			
Gln 81	7.17	7.11	3.92	1.54	2.24		NH_2 5.66, 5.32
				1.74	1.61		
Lys 82	7.88	7.35	4.06[o]	1.62	1.29		
				1.73			

Table I (Continued)

meso protons[p]	5	10	15	20
	9.85	9.34	9.34	9.22
ring methyls	2^1	7^1	12^1	18^1
	3.67	3.74	3.30	3.39
bridge methine	3^1	8^1		
	5.96	6.15		
bridge methyl	3^2	8^2		
	1.84	2.40		
propionates	**1a**	**1b**	**2a**	**2b**
13	4.26	4.57	2.67	3.43
17	4.68	3.90	3.35	2.72

[a] Values are in ppm at pH 3.5 unless stated otherwise. Main-chain NH resonances are reported at two temperatures. Other resonances are reported at 60 °C with exceptions that will be marked by footnotes. Most side-chain protons are relatively temperature insensitive. [b] Resolved at 32 °C to 2.91 and 2.93 ppm. [c] At 32 °C the spin system is 4.72, 2.48, 2.80 ppm. [d] Resolved at 32 °C to 1.62 and 1.70 ppm. [e] C_γ, C_δ, C_ϵ, and the amine protons were only observed at 32 °C. This appears to be a slowly exchainging amine in the protein. The side chain packs against the heme crevice near the more exposed heme propionate. It is possible that a salt bridge interaction slows exchange. [f] Shifts for C_β and the rest of the side chain are reported for 32 °C where the spin subsystem is best resolved. The C_α is temperature sensitive and has a shift value of 4.01 ppm at 60 °C. [g] At pH 4.6, 60 °C. At pH 3.5, C4 is 7.62 ppm, but C3, C5, C2, and C6 overlap at 7.69 ppm. [h] Resolved at 32 °C to 4.02 and 4.13 ppm. [i] The C_γ and C_δ protons of Ile 48 have been difficult to assign. They do not appear in COSY as a typical Ile spin system because the heme ring current seems to be shifting resonances out of the normal pattern into very crowded regions. There are strong NOE's from the nearby 20-meso-proton that implicate resonances at 1.01, 1.32, and 1.76 ppm to the Ile 48 spin system but do not identify them within it. The proposed assignment is tentative. [j] Resolved at pH 10.6 and 60 °C to 2.87 and 2.95 ppm. [k] Resolved at pH 10.6 and 60 °C to 2.87 and 2.95 ppm. [l] Resolved at pH 4.6 to 2.59 and 2.72 ppm. [m] Side chain at 32 °C. At 60 °C, the spin system overlaps with Lys 76. [n] Resolved at 32 °C to 3.96 and 4.01 ppm. [o] Temperature sensitive; 4.18 ppm at 32 °C. [p] Resolved at pH 10.6 and 32 °C; 5, 9.85 ppm; 10, 9.33 ppm; 15, 9.46 ppm; 20, 9.22 ppm.

Table II: Typical Chemical Shifts for Split Resonances in *P. aeruginosa* Cyt *c*-551 at pH 4[a]

	shift (ppm)	
proton	32 °C	60 °C
Ala 42 NH	7.84, 7.89	7.55, 7.59
Leu 44 NH	8.68, 8.71	8.49, 8.54
Ala 45 NH	8.41, 8.46	8.22, 8.27
Arg 47 NH	7.69, 7.73	7.53, 7.60
$N_\epsilon H$	7.31, 7.36	7.24, 7.30
Lys 49 NH	7.17, 7.20	7.06, 7.11
Gly 51 NH	7.45, 7.48	7.29, 7.34
Gln 72 NH	8.11, 8.16	8.04, 8.07
Ala 75 NH	8.84, 8.87	8.70, 8.74
Lys 76 NH	8.23, 8.29	8.09, 8.17

[a] This is an illustrative, not comprehensive, list. Other samples showed slightly different amounts of splitting and different affected resonances as discussed in the text.

shifts of resolved resonances for their later use as internal standards. DQF-COSY and NOESY spectra were obtained in ^2H_2O solutions, usually at 60 °C to take advantage of narrow lines. These spectra were used to assign aromatic side chains, heme resonances, and unusual resonances such as the iron ligands, Gly 24, and Pro 25. These spin systems became invaluable landmarks for the sequential assignment process. HOHAHA, SCUBA NOESY, and ECHO NOESY spectra were obtained on samples dissolved in 90% ^1H_2O with 10% ^2H_2O to provide spectrometer lock. To observe all the exchangeable amide protons, it was necessary to obtain spectra at pH 5 or below where the exchange rate is minimized. The HOHAHA spectra in combination with intraresidue NOE's determined the spin subsystems starting with the amide proton, then C_α, C_β, and so on. Because of limited digital resolution and the natural line widths of the protons, it was common for two or three amide protons to overlap in chemical shift. However, the amides are in general sensitive to temperature with variable behavior. By comparing two-dimensional spectra at 27, 32, 47, and 60 °C, the amides and their associated spin subsystems could be individually resolved when they were followed as a set. NOESY spectra at the different temperatures provided critical interresidue connectivities between NH(i) and NH($i + 1$), NH(i) and $C_\alpha(i - 1)$, NH(i) and $C_\beta(i - 1)$, and landmark resonances such as aromatic side chain and heme resonances. Figure 1 illustrates NOE's observed between amide protons for the N-terminal α-helix, and Table III summarizes some of the critical ones.

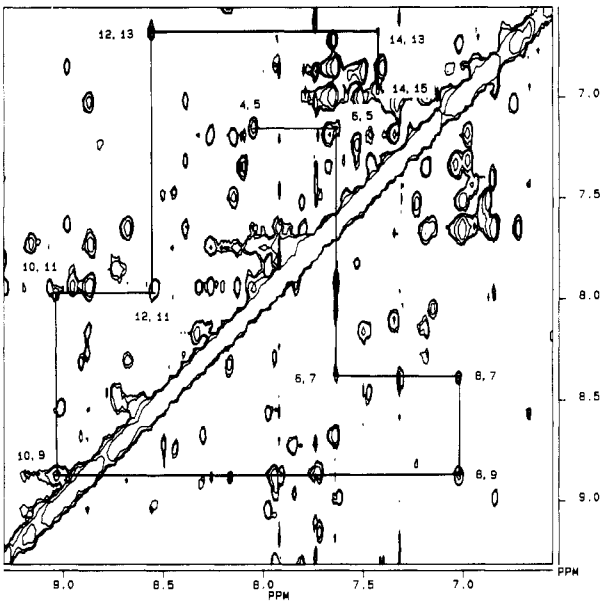

FIGURE 1: Portion of a NOESY spectrum of *P. aeruginosa* cyt *c*-551 at pH 4.6 and 32 °C showing the interresidue NH–NH NOE's used in the sequential assignment of the N-terminal α-helix. The relevant cross peaks are connected by the solid lines and are labeled with the residue numbers according to the convention that the first number is the residue whose NH chemical shift is given on the horizontal axis. The pattern begins with the cross peak 4,5, indicating an NOE between the NH of Glu 4 near 8 ppm and the NH of Val 5 near 7 ppm. The solid line connects the cross peak 6,5, indicating an NOE between Leu 6 and Val 5, and so forth.

Both the sequence and the crystal structure of *P. aeruginosa* cyt *c*-551 are known [see Matsuura et al. (1982) for details]. The heme group with IUPAC-IUB nomenclature is shown in Figure 2. The crystal structure was used as a tool to aid in the assignment process, subject to the following limitations. Protons were added to the carbon–nitrogen–oxygen skeleton of the crystallographic coordinates by the SYBYL software, consistent with standard bond geometries. For methyl groups, rotamer averages were used as necessary. Interproton distances were computed for nuclei initially assigned based upon observed NOE's and were qualitatively compared to the magnitude of the observed NOE. Quantitative interpretations were not attempted at this time. Substructures such as surface side

Table III: NOE Connectivity Diagram for *P. aeruginosa c*-551[a]

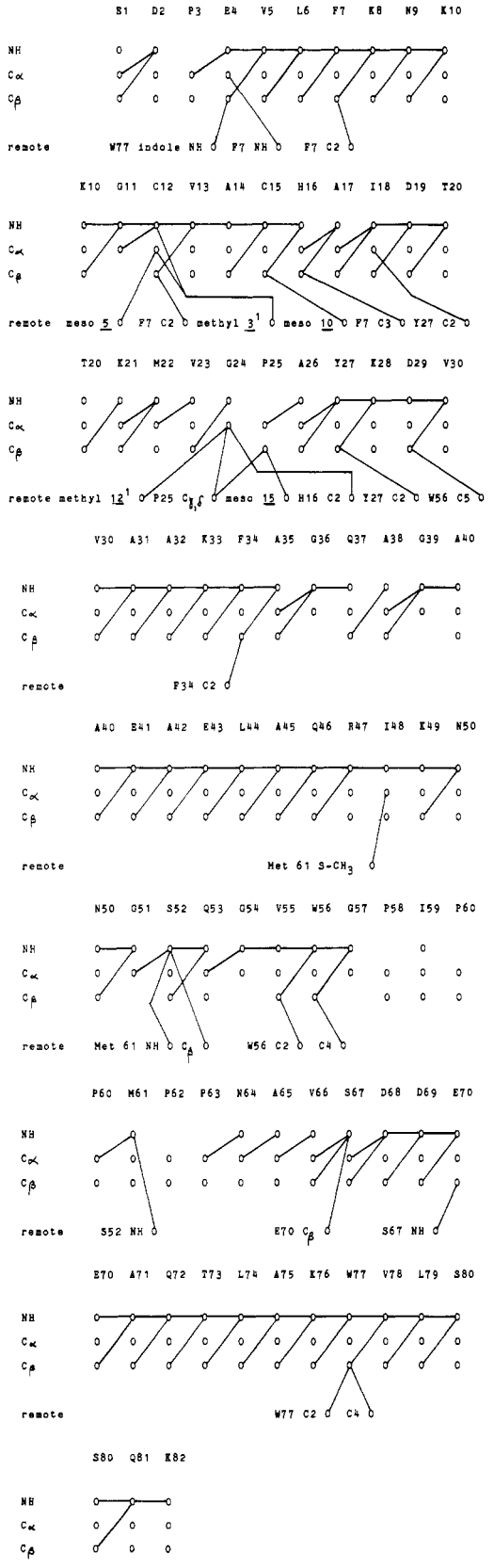

[a] The amino acids are listed with the single letter code. Under each the three circles represent the amide NH, C_α, and C_β. In the style of Wand et al. (1989), the solid lines represent a sequential or remote NOE observed in the assignment process. Intraresidue NOE's were observed, as well as NOE's to select C_γ and C_δ protons, but these are not listed here. Combined with DQF-COSY and HOHAHA relayed cross peaks, they served to define the spin subsystem of the individual residues. Not all NOE's are displayed, only those most critical for establishing identities.

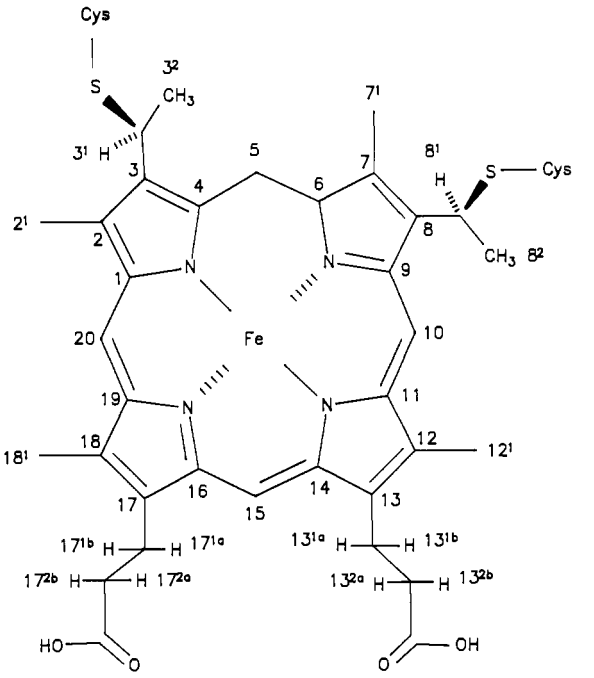

FIGURE 2: Heme group of *P. aeruginosa* cyt *c*-551 with the IUPAC-IUB nomenclature scheme.

chains, likely to be mobile, were not considered in this way. Although this might be considered as a bias to the spectral interpretation, to our knowledge there are no major contradictions between known crystal structures and NMR-deduced conformations for the same protein. The goal was to assign resonances and not treat the spectra as source for a de novo determination. The assigned resonances do reveal certain new features, which, while qualitatively consistent with the crystal data, were not revealed by the solid-state data.

The assignment process was complicated by the ring current of the heme, which shifted resonances to positions where chemical shift analogies were meaningless, and by the high percentage of proline residues (6 out of 82 residues), which break NH-related connectivities. In the crystal structure all proline residues are in the trans conformation. The NMR data were consistent with this because NOE's were observed between the α-proton of the preceeding residue and the δ-protons of the proline. This is how the δ-proton assignments were made for Pro 3, Pro 25, Pro 58, and Pro 62. The α-proton of Ile 59 may give rise to NOE's related to the δ-protons of Pro 60, but the region is crowded with NOE's due to Asn 9, Gly 11, and Trp 56 and assignment has not yet been accomplished. NOE's were observed between the α- and β-protons of proline residues and the succeeding main-chain amide, and this is how assignments were made for such protons in Pro 3, Pro 58, Pro 60, and Pro 63. The α and β proline protons also showed characteristic spin coupling patterns in scalar correlation spectra. The α and β assignments for Pro 62 are tentative. They were made on the basis of elimination, in that the spin subsystem was apparent in scalar correlation spectra and is characteristic of a proline side chain, and Pro 62 was the sole residue unaccounted for by other evidence. In principle the β- and δ-protons of all the prolines should be correlated by their spin coupling to the γ-protons, but the important cross peaks fall in the region around 2 ppm. This is so crowded that assignments could not be made, except for the special case of Pro 25 that will be discussed later.

There are eight side-chain amides in cyt *c*-551 from asparagine and glutamine residues. One was not observed, presumably because it exchanges too rapidly with water. The

other seven appeared strongly in HOHAHA spectra at acidic pH values and temperatures of 32 °C or lower, because of the strong geminal coupling between the inequivalent protons. The corresponding cross peaks are not prominent in DQF-COSY spectra, possibly because in the latter, the natural line width approaches the magnitude of the coupling constant and the antiphase nature of the lines causes cancelation. The amides of Asn 64 and Gln 81 where assigned on the basis of strong intraresidue NOE's to each other and to the β- and γ-protons. Asn 9, Asn 50, and Gln 53 were assigned in the same way, but in these cases the assignment is tentative because the NOE cross peaks were weak. There remain two unassigned amide systems as proton pairs at 7.45 and 6.71 ppm and at 7.31 and 6.77 ppm. The chemical shift of one of the Asn 64 NH_2 protons is unusual, 3.19 ppm. In the crystal structure, this proton packs against the heme in the crevice region, and so the low frequency shift is interpreted as due to a ring current shift by the heme. The amide protons assigned to Gln 81 at 5.66 and 5.32 ppm are both low in frequency. In the crystal structure they pack against the face of the Trp 77 indole ring where they may experience a ring current effect. In fact, there was a weak NOE from the 5.66 ppm resonance to the C4 proton of Trp 77.

Assignments are proposed in Table I. Not all side-chain protons could be followed in terms of scalar connectivity, presumably because the magnitude of the coupling constant (as determined by the dihedral angle) approached zero or the chemical shifts were so similar that cross peaks were not resolved from the diagonal. NOESY and COSY peaks in the crowded aliphatic regions were difficult to assign unambiguously. Proline γ-protons were especially troublesome in this manner. Different segments of the molecule have been assigned with different amounts of evidence. The helical segments, aromatic residues, and some unique residues near the heme have the highest confidence. The primary purpose of this report is to contrast aspects of the solution structure of *P. aeruginosa* cyt *c*-551 with its crystal structure and with the solution structure and NMR spectrum of the larger eukaryotic cyt *c*. For this purpose, the discussion will focus on residues and assignments made with high confidence. Studies are in progress to expand and confirm the assignments of Table I by studying the spectra of homologous proteins from other bacterial sources.

There are some nontypical chemical shifts in cyt *c*-551 compared to most proteins because of the heme ring current. These resonances are excellent probes of the heme crevice region, because their chemical shifts are highly sensitive to precise geometry with respect to the heme. Comparisons with the recently published assignments for horse and yeast ferrocytochromes *c* suggest that some of these may be considered as distinctive landmarks for cytochromes. The shifts of the ligand methionine have been discussed in detail from extensive one-dimensional studies (Senn et al., 1980). His 16 has a near normal C_α shift (3.64 ppm) but perturbed C_β shifts (0.87 and 0.21 ppm) due to the increased proximity to the heme ring. The corresponding protons in horse cyt *c* are at 3.65, 1.08, and 0.79 ppm, respectively. Gly 24 has a remarkable difference between the two C_α protons, 3.71 and 0.13 ppm. In horse cyt *c*, these are at 3.70 and −0.17 ppm. From the respective crystal structures, one α-proton is directly oriented toward the heme plane and the other out and away, accounting for the difference. The next residue, Pro 25 (Pro 30 in horse cyt *c*), has one C_β and C_γ directed toward the heme plane and the rest away, and this accounts for the observed spread in shifts. Two additional residues have abnormally low-frequency shifts for their C_α protons, Ile 48 (1.51 ppm) and Val 78 (2.60 ppm). Both are heme contact points from the crystal structure. In horse cyt *c*, the analogous residues are Leu 68 (3.12 ppm) and Leu 98 (3.46), which are low in frequency but not as low as for cyt *c*-551, indicating a different geometry with respect to the heme.

The assignments of Trp 56 and Trp 77 aromatic protons reverse earlier reports (Moore et al., 1977; Leitch et al., 1984) and should be explained. The original assignment was based on the reasonable argument that Trp 56 is closer on the whole to the heme than is Trp 77, and so its protons should be at lower frequency. Also the pattern of chemical shifts for the coupled resonances (doublet–triplet–triplet–doublet) matched that in horse cyt *c*. These turn out to be false leads. The pattern appears not to be a universal feature in both large and small cytochromes. Although on the whole, Trp 56 is closer to the heme than Trp 77, the C5 and C6 of Trp 77 point toward the heme plane and experience a bigger ring current, while those of Trp 56 point away. The new assignment is based upon multiple lines of evidence. The C2 and C4 of both tryptophans showed clear NOE's to C_β protons, and C4 of Trp 56 showed an NOE to C_α of Trp 56. These in turn were readily assigned by sequential and main-chain strategies. The aromatic protons also showed strong NOE's to many neighbor side chains, different and distinctive in each case. Especially compelling evidence was the following pattern of NOE's. C7 of each tryptophan showed strong NOE's to the indole NH. The indole NH of Trp 56 is the highest frequency proton, due in part to its location with respect to the heme edge. The indole NH's in turn showed strong NOE's to the respective C2 protons. The C2 of Trp 56 showed a strong NOE to the heme meso proton 15. This meso assignment has been firmly made in previous one-dimensional assignments and amply confirmed in the present study. The C2 proton also showed NOE's to the propionate protons as assigned in this study. Only Trp 56 is close to these unique protons.

As in the case of horse cyt *c*, aromatic side chains in cyt *c*-551 are largely interior (although edges may be solvent exposed). Crystallographic data for the solid state reported well-defined ring orientations. The solution-state NMR data provide evidence for benzoid ring mobility in cyt *c*-551, and as will be seen, this is a feature not completely in common with the larger horse cyt *c*. For a Tyr ring in a protein interior, in principal, the four ring protons can be chemical shift nonequivalently, while for a Phe ring all five could be nonequivalent. If there is motion about the C1–C4 axis, averaging converts the Tyr ring to an AA′XX′ subsystem as in the free amino acid. Since different couplings to other spins are not observable in protein spectra because of the natural line widths and limited digital resolution, AA′ appears as A2 etc. Examples of this type of mobility have been documented for lysozyme (Campbell et al., 1975) and basic pancreatic trypsin inhibitor (Wüthrich & Wagner, 1975). In cyt *c*-551, the ring of Tyr 27 was observed as an A_2X_2 spin system, that for Phe 7 as AM_2X_2, and that for Phe 34 as AB_2C_2. This is illustrated for Phe 34 in Figure 3. These spin patterns persisted from 60 to 4 °C and pH 3.5 to 10.6, and so we consider it unlikely that there is accidental degeneracy of nonaveraged spin systems. For ring motion, there are two possibilities: 180° flips between two relatively fixed orientations and rotation with no strongly perferred orientation. We tentatively prefer the interpretation of 180° flips, because the equivalent protons (C2 + C6 and C3 + C5) show strong NOE's to neighbors. For example, C6 of Tyr 27 is 2.9 Å from an Ile 18 methyl in the crystal structure and there was a strong NOE involving these

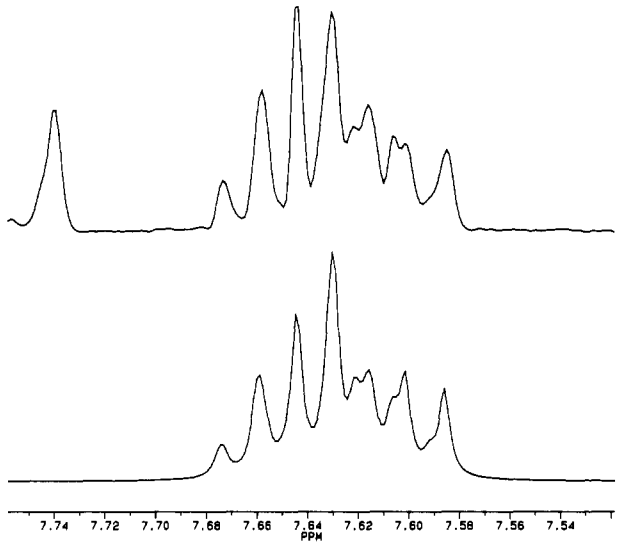

FIGURE 3: Spin system of the aromatic ring of Phe 34. The top trace shows a portion of the spectrum of *P. aeruginosa* cyt *c*-551 at pH 4.6 and 60 °C in deuterium oxide buffer where the amide protons have been exchanged. The singlet at 7.74 ppm is from the C2 proton of Trp 56. The bottom trace is a spectrum simulation where C2 has been made equivalent to C6 at 7.63 ppm, C3 has been made equivalent to C5 at 7.66, and C4 is at 7.62 ppm. The coupling constant between C2 and C3 was 7.87 Hz and between C3 and C4, 7.80 Hz. A Lorentzian line width of 1.7 Hz was employed. The spectra on the low-frequency side also contain a multiplet for the C7 proton of Trp 56, which is spin coupled to C6 with a coupling constant of 7.8 Hz. The multiplet for C6 is outside the displayed region. Slight mismatch between the traces is believed to be due to residual amide proton intensity.

protons. Numerous such NOE's were observed. If mobility corresponded to constant rotation, the average distance to neighboring side chains would be larger than the crystal structure, multiple transfer pathways would exist, and these strong NOE's would not be expected.

The sequence and tertiary structure analogue of Phe 7 (*c*-551) in horse cyt *c* is Phe 10 and it shows a nonmobile ring with clearly resolved resonances at 7.17 (C2), 7.18 (C6), 6.98 (C3), and 6.12 (C5) ppm. Because of deletions, there is no sequence homologue of Phe 34 or Tyr 27 in horse cyt *c*, but Tyr 48 and Phe 36 respectively are tertiary homologues according to the crystal structures. Tyr 48 (horse) is also nonmobile with resolved resonances at 7.99 (C2), 7.51 (C6), 7.09 (C3), and 7.29 (C5) ppm. Phe 36 (horse) is mobile just as Tyr 27 (*c*-551). However, the chemical shifts of Phe 36 (horse) C2 + C6 (7.37 ppm) and C3 + C5 (6.88), when compared to Tyr 27 (*c*-551) at 5.78 and 4.63 ppm, reflect the fact that in solution Tyr 27 in cyt *c*-551 must pack closer to the heme plane and experience larger ring current effects. In the crystal structures, Phe 36 C3 (horse) comes within 7.5 Å of the heme methyl 18^1, while Tyr 27 C3 (*c*-551) comes within 3.9 Å of this methyl group. Other aromatics in horse cyt c for which there are no homologues in cyt *c*-551 are a mixture of mobile and nonmobile. Ring mobility at related positions appears to be a clear distinction between the smaller prokaryotic cyt *c*-551 and the larger eukaryotic horse cyt *c*. Perhaps in cyt *c*-551 there is just insufficient bulk to constrain a single orientation.

Many heme resonances have been assigned in cytochromes, but data have been lacking for the propionic acid substituents. Figure 4 illustrates the geminal and vicinal coupling patterns observed in DQF-COSY spectra that provided evidence for the assignment for cyt *c*-551. The 13^1- 17^1-protons for the propionates at 4.26, 4.57, 4.68, and 3.90 ppm have chemical shifts (4.22 ppm for free heme) similar to α-carbon protons, but they are unique in showing geminal as well as vicinal coupling to protons at lower frequency corresponding to the 13^2- and 17^2-methylenes at 2.67, 3.43, 3.35, and 2.72 ppm (3.14 ppm for free heme). Each geminal proton shows only one cross peak to a scalar-coupled vicinal proton, because the dihedral angle to the other is ca. 80–90° and the coupling constant is near zero. In NOESY spectra, the 15-meso-proton at 9.34 ppm shows strong cross peaks to the propionate-assigned peaks shown in Figure 4. The respective assignments in cyt *c*-551 to the inner and outer propionates were accomplished by NOE's between the inner propionate protons 17^{1a}, 17^{1b}, and 17^{2b} and the indole NH of Trp 56, which is close in crystal structure only to this inner propionate. This spin system and similar shifts have been observed in another bacterial cytochrome currently under study in our group. The propionates were not reported in horse or yeast cytochromes *c* (Wand et al., 1989; Pielak et al., 1988). Forearmed with the results from cyt *c*-551, it was possible to observe corresponding spins in horse cyt *c* at pH 7 in deuterium oxide buffer at 60 °C. In the DQF-COSY spectrum of horse cyt *c* there are three resolved cross peaks with large coupling constants at (4.17, 2.64 ppm), (3.16, 2.64 ppm), and (3.84, 2.67 ppm) that cannot be assigned on the basis of the protons reported by Wand et al. [see Table I, Wand et al. (1989)]. The first and third are interpreted as due to vicinal propionate couplings, while the second is due to a geminal coupling. The rest of the coupling pattern is obscured by overlap with other nonrelated COSY cross peaks, but these are sufficient to mark five out of the eight possible propionate chemical shifts as 4.17, 3.84, 3.16, 2.67, and 2.64 ppm. In NOESY spectra the 15-meso is readily assigned on the basis of distinctive cross peaks to other heme resonances. The 5-meso (9.30 ppm) shows NOE's to the 3-methine (5.25 ppm) and the 7-methyl (3.80 ppm); the 10-meso (9.54 ppm) to the 8-methine (6.30 ppm), the 8-methyl (2.58 ppm), and the 12-methyl (3.56 ppm); and the 20-meso (9.25 ppm) to the 2-methyl (3.48 ppm) and the 18-methyl (2.17 ppm). The critical confirming assignment data are that the 15-meso (9.61 ppm) shows NOE's to the propionate peaks at 4.17, 3.84, 3.16, and 2.67 ppm.

The two heme propionate side chains in cyt *c*-551, as in other cytochromes, are buried in the protein interior. The 13-propionate is called the "outer", since it is close to the surface and may be partially exposed. The 17-propionate, or "inner", is hydrogen bonded to Trp 56 and Arg 47. Matsuura et al. (1982) suggested the outer propionate as the one susceptible to protonation because of its relative exposure. Leitch et al. (1984, and references therein) concluded that protonation of the inner propionate was responsible for the oxidation potential dependence of cyt *c*-551 and the structural transition that occurs with p*K* around 7. The high p*K* for a carboxylate may be rationalized by considering that the hydrophobic environment in the heme crevice perturbs the p*K* to an abnormal value. Eukaryotic cytochromes do not show oxidation potential or structural transitions around neutral pH. The supporting evidence for the conclusions of Leitch et al. may be criticized on the following grounds. One line of evidence relied upon a chemical shift dependence for two resonances in ferricytochrome *c*-551 that were assigned to geminal propionate methylene protons. These were assigned to the inner propionate based upon an NOE to C2 of Trp 56. However, C2 is also close to methylene protons on the outer propionate, so the assignment is actually ambiguous. In the present study of the ferrocytochrome, we observed NOE's from this C2 to both propionates. Furthermore, although their assignment of the C2 singlet of Trp 56 was correct, the rest of the ring protons were reversed between 56 and 77. Assignments based

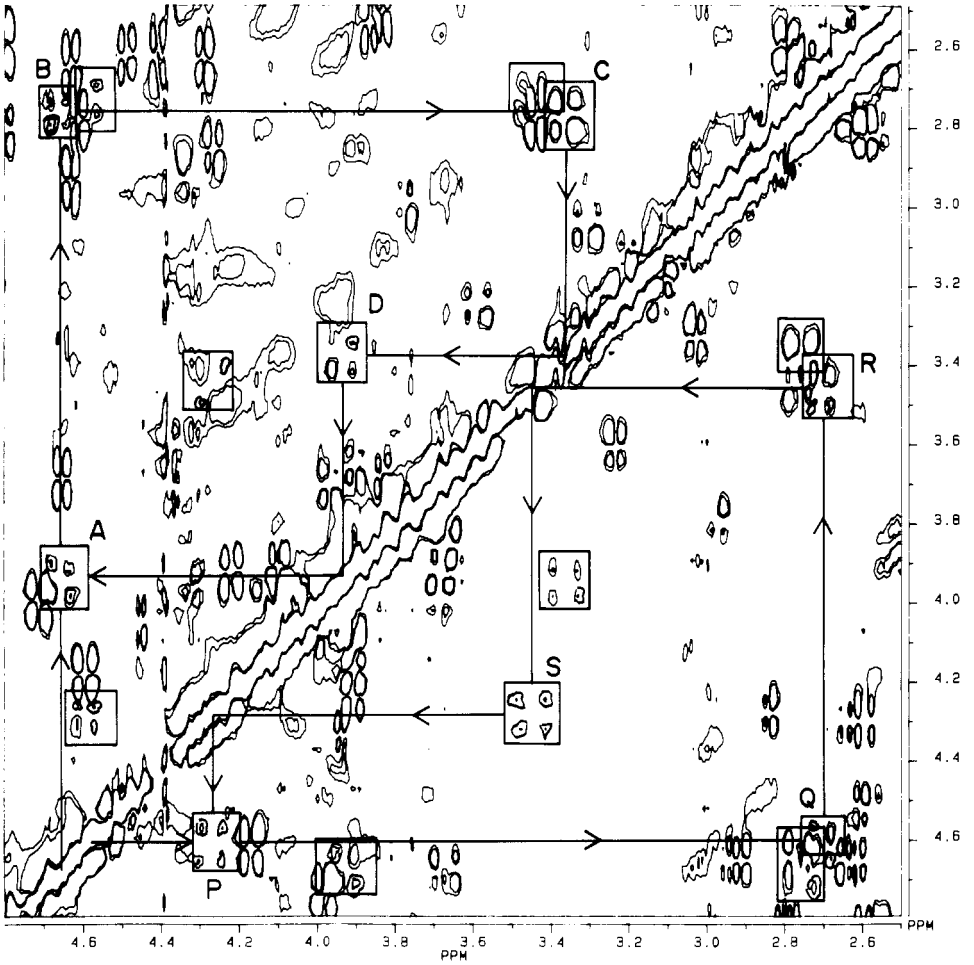

FIGURE 4: Scalar coupling patterns observed in a DQF-COSY spectrum of *P. aeruginosa* cyt *c*-551 for the proposed propionate methylene protons. The spectrum was in deuterium oxide at pH 4 and 60 °C. Positive and negative contours have been plotted without discrimination. The pattern above the diagonal has been traced for the 17-methylene protons. The solid line starts out on the diagonal at 4.65 ppm (17^{1a}) and goes to the cross peak marked A, which is due to geminal coupling between 17^{1a} and 17^{1b}; then it goes to the cross peak, B which is due to vicinal coupling between 17^{1a} and 17^{2b}, then to cross peak C due to geminal coupling between 17^{2b} and 17^{2a}, then to the diagonal at 17^{2a}, then to the cross peak D due to vicinal coupling between 17^{1b} and 17^{2a}, then to the diagonal at 17^{1b}, and finally back to the cross peak A due to geminal coupling between 17^{1a} and 17^{1b}. Below the diagonal, cross peaks P, Q, R, and S mark the same pattern but for the 13-propionate. Symmetry-related cross peaks have been marked with a box on both sides of the diagonal. The symmetry is only approximate because data were collected with unequal digital resolution in F2 and F1.

upon select resolved ferricytochrome resonances are risky, because, the other unresolved propionate protons may have even larger chemical shift dependences on pH. Complete interpretations of paramagnetic shifts are difficult. For example, the heme methyl group 18 is the ring methyl closest to the inner propionate, and its chemical shift in the ferricytochrome is insensitive to pH. The other main line of argument relied upon complex considerations of the behavior of chemically modified His 47 in the related cyt *c*-551 from *P. stutzeri*. These considerations relied upon the implicit assumptions that His 47 in *P. stutzeri* hydrogen bonds to the inner propionate in the same manner as Arg 47 in *P. aeruginosa*, and that the modification does not radically disrupt the surroundings. These are reasonable assumptions, but the inverse tenets cannot be totally excluded.

Further evidence is thus needed to resolve the question of what is protonated in cyt *c*-551 with a p*K* near 7. The indole NH of Trp 56 is hydrogen bonded to a carbonyl oxygen on the inner propionate in the crystal structure and shows NOE's to the propionate methylene protons in NOESY spectra. As shown in Figure 5, the chemical shift has a strong sensitivity to pH with a p*K* near 7. The indole NH of Trp 77 also shows a modest pH dependence with a p*K* near 4. This latter effect is ascribed to the protonation of the surface-exposed Glu 4 that is near to Trp 77. The behavior of Trp 56 supports the conclusion of Leitch et al. (1984). One would expect that the propionate methylenes on the inner propionate would also show a stronger sensitivity to pH than the methylenes on the outer propionate, but the behavior of these protons turns out to be ambiguous. As shown in Figure 5, the inner propionate proton 17^{1a} does shift about 0.15 ppm to lower frequency when going from pH 4 to 9, while the outer propionate proton 13^{1a} shifts by less than 0.03 ppm. But 17^{1b} shifts by only 0.03 ppm to higher frequency, 17^{2a} shifts by 0.06 ppm to lower frequency, and 13^{2a} shifts by 0.05 ppm to higher frequency over the same pH range. Thus there is a mixture of effects at both propionates, with only a slightly greater sensitivity of the inner propionate. The chemical shifts of the propionate protons were most accurately measured from NOESY cross peaks to the 15-meso-proton, and so data for only five of the eight were considered reliable.

What is the expected effect on the propionate methylene chemical shifts upon protonation of the carboxylates? For the carbon monoxy complex of free ferrous heme b in the mixed solvent dimethyl sulfoxide/water, upon changing from acidic to basic conditions, the methylene protons 13^2 and 17^2 (adjacent to the carboxylate) moved to lower frequency by 0.31 ppm and the 13^1- and 17^1-protons moved to lower frequency by 0.14 ppm. In free heme the two propionates are degenerate in chemical shifts. While free heme in dimethyl sulfoxide/

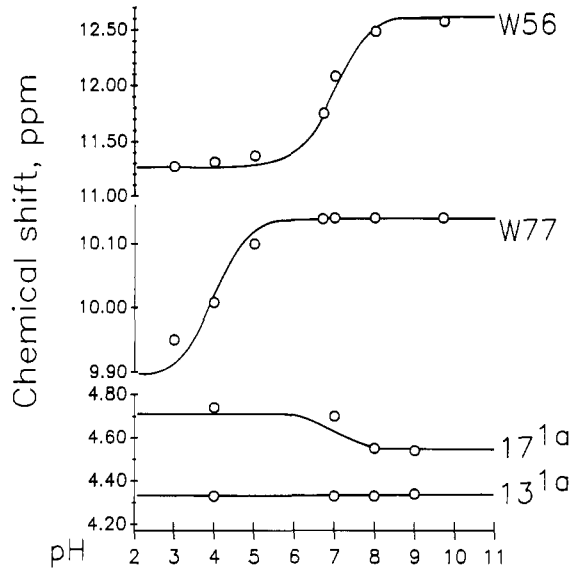

FIGURE 5: Chemical shift dependence on pH for select resonances in *P. aeruginosa* cyt *c*-551. The indole NH of Trp 56 and Trp 77 are plotted along with two propionate methylene protons. The indole protons are resolved in one-dimensional spectra and can be followed readily at multiple pH values. As explained in the text, shifts for the propionate protons were determined from NOESY cross peaks. Note that the vertical scale is broken. On each scale 1 tick mark represents 0.1 ppm, but the scale for individual protons has separate vertical expansions. The Trp 56 indole proton shifts 1.5 ppm; Trp 77 indole NH 0.2 ppm; 17^{1a} 0.15 ppm; and 13^{1a} less than 0.03 ppm. The curves through the data points for Trp 56 (labeled W56) and the 17^{1a}-methylene proton correspond to a pK of 7.0, the curve through Trp 77 (W77) corresponds to a pK of 4.0, and a straight line has been shown for 13^{1a}.

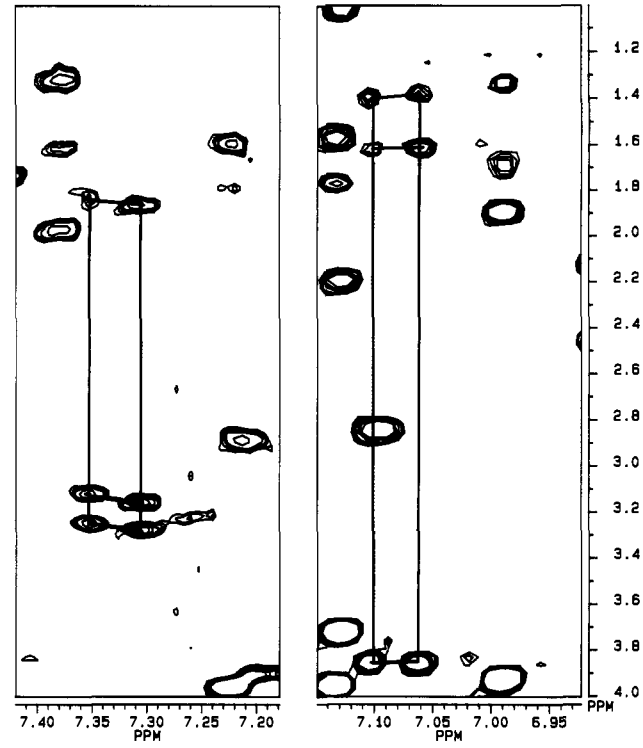

FIGURE 6: Heterogeneity of spin systems in *P. aeruginosa* cyt *c*-551. The two panels are sections of HOHAHA spectra taken with 55-ms spin-locking periods so that relayed coupling may be seen. The vertical lines connect coupled spins, while the approximate horizontal lines connect chemical shifts between the two sets that are interpreted as due to different conformations. The right panel is from a spectrum taken at 60 °C and shows cross peaks due to Lys 49 at ca. 7.08 ppm and 3.85 ppm due to coupling between the backbone NH and C_α and then relayed to C_β protons at ca. 1.5 ppm. The left panel is from a spectrum at 32 °C and shows cross peaks due to Arg 47 at about 7.3 and 3.2 ppm due to coupling between the side chain N_ϵ and the C_δ protons, relayed to C_δ at about 1.8 ppm. The two different temperatures were chosen for display because at these there is minimum overlap with other spin systems and the duplication is most obvious.

water may not be a perfect model for the heme crevice in cyt *c*-551, it was surprising that the protein case showed smaller shifts and shifts in the opposite direction.

The behavior of the side chain of Arg 47 provided additional evidence that the inner propionate is the protonation site. Upon going from pH 4 to 9, the $N_\epsilon H$ shifts from 7.27 ppm (27 °C) to 8.21 ppm with an apparent pK of 7. Like Trp 56, Arg 47 is hydrogen bonded to the inner propionate, but to the opposite oxygen. The high sensitivity to pH is consistent with protonation of the inner propionate.

Three other backbone NH resonances that showed very large pH dependences for their chemical shifts were Ser 67 NH, Glu 4 NH, and Asp 2 NH. The chemical shift of Ser 67 NH changes from about 9.2 ppm at pH 7 to 8.5 ppm at pH 3.5; Glu 4 changes from 8.3 to 7.9 ppm; and Asp 2 changes from 9.2 to 8.9 ppm. A complete titration curve could not be obtained, because the protein was unstable at more acidic values, but the behavior was indicative of a pK in the range 3.8–4.4. In the crystal structure, Ser 67 NH is hydrogen bonded to the carbonyl of the side chain of Glu 70, so that the NMR behavior appears to reflect the protonation of this side chain. Similarly, the behavior of the other two resonances may reflect their side-chain protonation.

An interesting phenomenon was observed over the course of this study as a consequence of observing many different samples at a variety of pH values. Some two-dimensional spectra were complicated by the observation of more NH resonances than could be accounted for in an 82-residue protein. The protein was known to be pure. Gel electrophoresis showed a single band and spectra in ^2H_2O showed only the expected resonances. The extra resonances appeared as a duplication or splitting of the spin subsystems connected with a given NH resonance as would be observed in the fingerprint region. The type of pattern is illustrated in Figure 6. The splitting was most pronounced in terms of the shift of the amide position, with C_α and other nonlabile protons showing very slight or no chemical shift difference. This has been interpreted as the existence of two possible conformations for the associated protons. The resonances affected were in the 40's helix, which forms the heme crevice at the bottom near the propionates (especially 44, 45, 47, 49, 51); Ser 67, which is at the beginning of the C-terminal helix; then the C-terminal helix from 71 to 77 at the back of the heme crevice region; and finally the initial portion of the N-terminal helix (especially Asp 2, Glu 4, and Val 5), which packs against the helix from 71 to 77. The side chains of 74 and 75 also pack against the inner propionate. Chemical shift differences for two sets from a single sample at pH 4 are summarized in Table II. Several points may be made. The splitting is not present in freshly prepared samples. The half-time for the appearance has not yet been systematically measured, because it is so slow. The two sets were usually close to equal intensity, although in some cases one set could appear stronger. The differences were not large, less than 0.1 ppm in most cases, but still larger than the maximum possible NH vicinal coupling constant. The most seriously split resonances observed were Asp 2, Glu 4, and Ser 67. These complications are not evident in one-dimensional spectra, and key resonances such as the Met 61 side chain, the meso protons, and the aromatic rings do not show any splitting. The splittings appear to be a consequence of the age of the sample and its precise history of handling, especially in terms of temperature and pH to which it has been

exposed. We have not yet determined all the factors that control the splitting, and different samples can show a different degree of splitting and the number of resonances from the above sets that are affected. The two conformations that correspond to the two sets in a split resonance must be in slow exchange, if at all, on the NMR time scale, because two discrete sets were observed with approximate line widths comparable to other resonances. We have been unable to date to interpret any major differences in NOE's involving split resonances that might lead to a simple identification of the structure difference in the two conformations. It is likely to be a very modest change, such as a shift of a fraction of an angstrom of the helical segments. Studies are in progress to determine reproducible conditions that will cause the splitting, and then a quantitative interpretation of NOE differences may reveal more precise details. Since the most affected resonances are in proximity with the inner propionate and the surrounding heme crevice, one can hypothesize that two conformations exist around this site that are approximately equal in stability but separated by a modest energy barrier. Elevated temperature, acidic pH, or just time may cause the barrier to be crossed by a portion of the molecules.

A single sample that showed the splitting was opened to the atmosphere, reoxidized, and rechromatographed on (carboxymethyl)cellulose. Ion-exchange chromatography of *P. aeruginosa* cyt *c*-551 always produces a small amount of denatured material that binds irreversibly to the column. This probably arises because of the pH adjustments to the sample and the acidic value, pH 3.9, at which the column is eluted. As mentioned previously, the oxidized form is not as stable as the reduced. Except for the denatured material, only a single chromatographic band was observed. This sample was prepared for NMR spectroscopy as with freshly isolated protein, and a HOHAHA spectrum was recorded at pH 4 and 32 °C. The splitting was not present and the spectrum was indistinguishable from that obtained with freshly isolated protein. It may be the case that in the oxidized form or during binding to the support, the different conformations converge back to the original.

Summary

Two-dimensional NMR spectroscopy has been used to assign the main-chain and majority of the side-chain protons in the reduced form of *P. aeruginosa* cyt *c*-551. The assignments, when compared to assignments from other cytochromes, help to establish that there are resonances with atypical chemical shifts that arise because of the strong ring current due to the heme in both prokaryotic and eukaryotic versions. In cyt *c*-551 these involve protons in the ligands His 16 and Met 61 and then Gly 24, Pro 25, Tyr 27, Ile 48, and Gly 51. They have chemical shifts of unusually low frequency because of their proximity to the heme plane. As such, they are excellent probes of the structural intergrity around the heme crevice. For example, if a chemically modified protein or a mutant were examined, changes in these probe resonances could help to determine any reorganization around the heme. There are some resonances found in cyt *c*-551 that are unique to this smaller cytochrome. These include the proline resonances adjacent to the ligand Met 61 and the amide NH_2 protons of Asn 64 and Gln 81. The latter have unusual chemical shifts because of proximity to the heme and Trp 77, respectively. Examination of the pH behavior of resonances in cyt *c*-551 associated with Trp 56, Trp 77, Arg 47, and the heme propionates confirms the conclusions of Leitch et al. (1984) that the inner, or buried, propionate titrates with a pK near neutrality. In *c*-551, benzoid aromatic side chains in the protein interior are undergoing rapid 180° flips. In contrast, in the eukaryotic cytochromes, there are both rapid and slow or immobile aromatic rings. Over a period of time in the reduced state, cyt *c*-551 may develop conformational heterogeneity. This becomes evident by a splitting of resonances of main-chain amides. The actual structural difference has not yet been determined but is likely to be a very modest rearrangement involving residues in the N- and C-terminal helices and the 40's helix.

Acknowledgments

The authors are grateful to Drs. A. J. Wand and W. S. Englander for discussion of their results on horse cyt *c* and Drs. A. M. Gronenborn, G. M. Clore, and P. C. Driscoll for invaluable technical advice on optimizing the performance of our spectrometer. Tripos Associates, Inc., St. Louis, MO, provided support for the SYBYL macromolecular modeling software.

Registry No. Cyt *c*-551, 9048-77-5; propionic acid, 79-09-4.

References

Almassy, R. J., & Dickerson, R. E. (1978) *Proc. Natl. Acad. Sci. U.S.A. 75*, 2674–2678.
Ambler, R. P. (1963a) *Biochem. J. 89*, 341–349.
Ambler, R. P. (1963b) *Biochem. J. 89*, 349–378.
Bax, A., & Davis, D. G. (1985) *J. Magn. Reson. 65*, 355–360.
Brown, S. C., Weber, P. L., & Mueller, L. (1988) *J. Magn. Reson. 77*, 166–169.
Campbell, I. D., Dobson, C. M., & Williams, R. J. P. (1975) *Proc. R. Soc. London, Ser. B 189*, 503–509.
Chao, Y. H., Bersohn, R., & Aisen, P. (1979) *Biochemistry 18*, 774–779.
Dickerson, R. E., & Timkovich, R. (1975) in *The Enzymes* (Boyer, P. O., Ed.) pp 397–547, Academic Press, New York.
Dickerson, R. E., Timkovich, R., & Almassy, R. J. (1976) *J. Mol. Biol. 100*, 473–491.
Driscoll, P. C., Clore, G. M. Beress, L., & Gronenborn, A. M. (1989) *Biochemistry 28*, 2178–2187.
Englander, S. W., & Wand, A. J. (1987) *Biochemistry 26*, 5953–5958.
Hoult, D. I., Chen, C. N., Eden, H., & Eden, M. (1983) *J. Magn. Reson. 51*, 110–117.
Keller, R. M., & Wüthrich, K. (1976) *FEBS Lett. 70*, 180–183.
Keller, R. M., & Wüthrich, K. (1978) *Biochem. Biophys. Res. Commun. 83*, 1132–1139.
Leitch, F. A., Moore, G. R., & Pettigrew, G. W. (1984) *Biochemistry 23*, 1831–1838.
Macura, C., Huang, Y., Suter, D. & Ernst, R. R. (1981) *J. Magn. Reson. 43*, 259–281.
Marion, D., & Wüthrich, K. (1983) *Biochem. Biophys. Res. Commun. 113*, 967–974.
Marion, D., & Bax, A. (1988) *J. Magn. Reson. 79*, 352–356.
Matsuura, Y., Takano, T., & Dickerson, R. E. (1982) *J. Mol. Biol. 156*, 389–409.
Meyer, T. E., & Kamen, M. D. (1982) *Adv. Protein Chem. 35*, 105–212.
Moore, G. R., & Williams, R. J. (1977) *FEBS Lett. 79*, 229–232.
Moore, G. R., Pitt, R. C., & Williams, R. J. P. (1977) *Eur. J. Biochem. 77*, 53–60.
Moore, G. R., Pettigrew, G. W., Pitt, R. C., & Williams, R. J. P. (1980) *Biochim. Biophys. Acta 590*, 261–271.
Pielak, G. J., Boyd, J., Moore, G. R., & Williams, R. J. P. (1988a) *Eur. J. Biochem. 177*, 167–177.

Pielak, G. J., Atkinson, R. A., Boyd, J., & Williams, R. J. P. (1988b) *Eur. J. Biochem. 177*, 179–185.
Rance, M., Sorensen, O. W., Bodenhausen, G., Wagner, G., Ernst, R. R., & Wüthrich, K. (1984) *Biochim. Biophys. Acta 117*, 479–485.
Senn, H., Keller, R. M., & Wüthrich, K. (1980) *Biochem. Biophys. Res. Commun. 92*, 1362–1369.
Sklenar, V., & Bax, A. (1987) *J. Magn. Reson. 74*, 469–479.
Timkovich, R. (1979) in *The Porphyrins* (Dolphin, D., Ed.) pp 241–294, Academic Press, New York.
Timkovich, R. (1986) *Biochemistry 25*, 1089–1093.
Timkovich, R., Dhesi, R., Martinkus, K. M., Robinson, M. K., & Rea, T. (1982) *Arch. Biochem. Biophys. 215*, 45–58.
Timkovich, R., Cai, M. L., & Dixon, D. W. (1988) *Biochem. Biophys. Res. Commun. 150*, 1044–1050.
Wand, A. J., DiStefano, D. L., Feng, Y., Roder, H., & Englander, S. W. (1989) *Biochemistry 28*, 186–194.
Wüthrich, K. (1986) *NMR of Proteins and Nucleic Acids*, pp 40–202, Wiley-Interscience, New York.
Wüthrich, K., & Wagner, G. (1975) *FEBS Lett. 50* 265–268.

Resonance Raman Studies of Hemoglobins Reconstituted with Mesoheme. Unperturbed Iron–Histidine Stretching Frequencies in a Functionally Altered Hemoglobin†

Shanthini Jeyarajah and James R. Kincaid*
Chemistry Department, Marquette University, Milwaukee, Wisconsin 53233
Received December 8, 1989; Revised Manuscript Received February 16, 1990

ABSTRACT: Hybrid hemoglobins, containing mesoheme in one type of subunit and protoheme in the partner subunits, have been studied by resonance Raman spectroscopy. These hybrids have been studied in both the met hybrid and fully reduced, deoxy forms. Judicious choice of laser excitation frequency permits selective enhancement of modes associated with each type of subunit; i.e., either meso- or protoheme-containing subunit. The assignments of low-frequency modes of meso- and protoheme are briefly discussed with special reference to the iron–histidine linkage. Despite functional differences between the hybrids, no significant changes in the strength of the iron–histidine linkages are detected by resonance Raman spectroscopy. These results are discussed with reference to recent high-resolution NMR studies of these same hybrids.

The mechanism of hemoglobin (Hb) cooperativity continues to occupy a prominent position as a subject of interest in biophysical research (Antonini et al., 1981; Baldwin, 1975; Ackers & Smith, 1987). Despite a considerable effort by many research groups and an impressive history of accomplishment, precise definition of the stereochemical mechanisms by which ligand binding to one subunit affects the reactivity of the partner subunits remains elusive. In addition to structural and functional characterization of the native protein, the characterization of biologically (i.e., mutant) and chemically modified derivatives represents a useful approach to investigate these mechanisms (Imai, 1985; Pettigrew et al., 1982; Simolo et al., 1985). Specific interactions of the prosthetic group (heme) substituents with surrounding protein residues has not been overlooked (Sono & Asakura, 1974; Seybert et al., 1976; Chang et al., 1984; Kawabe et al., 1982; Makino & Sugita, 1978). In fact, elegant calculations carried out by Karplus and co-workers support convincing arguments for the importance of specific substituent–residue interactions (Gelin et al., 1983). Thus, hemoglobin has been reconstituted with a variety of hemes bearing a number of different substituents and the functional properties of these derivatives have been carefully documented. While such functional characterization studies are essential for establishing the effectiveness of a particular chemical modification in altering ligand-binding properties, it is important to document modification-induced perturbations in structure and bonding at key sites within the tetramer in order to gain insight into the structural basis for the effect. It is only relatively recently that sophisticated structural probes of the heme and its surroundings have been developed, two of the most powerful of which are nuclear magnetic resonance (NMR) (Lamar, 1979; Ho & Russu, 1981) and resonance Raman (RR) spectroscopies (Kitagawa, 1986; Spiro, 1985; Rousseau & Friedman, 1988; Yu, 1986).

Thus far, only one report has appeared in which NMR was used to provide complementary active-site structural characterization of a hemoglobin derivative containing a selectively modified heme. Thus, Ishimori and Morishima (1986) have described thorough NMR spectroscopic studies of deuteroheme and mesoheme derivatives of Hb; i.e., $(\alpha_m\beta_p)_2$, $(\alpha_p\beta_m)_2$, $(\alpha_m\beta_m)_2$, and $(\alpha_d\beta_d)_2$ [where the d and m subscripts designate a deuteroheme- or mesoheme-containing subunit and the p subscript indicates that the subunit contains the (native) protoheme prosthetic group].

In this report we present results of corresponding RR studies of mesoheme-reconstituted Hb derivatives as the deoxy tetramers and metcyano hybrids. Judicious choice of laser excitation wavelength permits selective enhancement of the individual subunits in the fully deoxy hybrids and reveals iron–histidine stretching frequencies that are not substantially different from those of the native system.

Experimental Procedures

Preparation of Hb Derivatives. Mesohemin chloride was purchased from Mid Century Chemical Co., Posen, IL, and used as received. All samples were found to be pure as determined by pyridine hemochromogen spectra (Smith, 1975) and thin-layer chromatography (DiNello & Dolphin, 1975) (single spot).

† This work was supported by a grant from the National Institutes of Health (DK 35153 to J.R.K.).

0006-2960/90/0429-5087$02.50/0